A Finite Difference Time Domain Method for Passive Intermodulation Analysis of Nonlinear Metal-Metal Contact

Tuanjie Li [1], Wangmin Zhai [1], Xiangyang Li [1], Xiaofei Ma [2], and Jie Jiang [3]

[1] School of Mechano-Electronic Engineering
Xidian University, Xi'an, 710071, China
tjli888@126.com, wang0min@163.com, 1950973447@qq.com

[2] Xi'an Institute of Space Radio Technology
Xi'an, 710000, China
maxf041600@sina.com

[3] Honghe University
Mengzi, 661100, China
jiangjie_uoh@163.com

Abstract ─ The passive intermodulation (PIM) has gradually become a serious electromagnetic interference in the high-power and high-sensitivity RF/microwave communication system with the existence of the nonlinear metal-to-metal (MM) contacts. This paper proposes a finite difference time domain (FDTD) method for PIM analysis of nonlinear MM contacts. There are two kinds of models, the power series model and the equivalent circuit model, to describe the nonlinear MM contacts. Then the FDTD method is applied to analyze the nonlinear models so that the nonlinear current through the MM contact can be determined. For the microwave transmission devices, the PIM power level can be obtained by fast Fourier transform of the nonlinear current. For the microwave radiation devices such as antennas, the nonlinear currents are taken as a new electromagnetic transmitting source, the far-field scattering and PIM power level can be obtained by the FDTD method. Finally, a comparison between the simulation and experimental results is illustrated to verify the validity of the proposed method.

Index Terms ─ Equivalent circuit model, metal-to-metal contact, passive intermodulation, power level, power series model, time domain finite difference method.

I. INTRODUCTION

With the development of higher power, wider band, and higher receiving-sensitivity communication systems, the passive intermodulation (PIM) has become a serious problem that cannot be ignored because PIM noise signals will fall into the receiving band [1]. The passive intermodulation products (PIMP) are generated for the inherent nonlinear I-V response curve of passive devices. When the nonlinear passive devices are excited by two- or multi-carriers, many intermodulation distortion signals are generated in the system. Basically there are two types of passive nonlinearities in communication system: contact nonlinearity and material nonlinearity [2]. The existing researches showed the nonlinear metal-to-metal (MM) contact is one of potential PIM sources in passive devices. Up to now, two mathematical models have been proposed to describe the nonlinear MM contacts. One is the power series model applied to represent the nonlinear I-V response curve of the MM contacts [3, 4]. The other is the equivalent circuit model applied to reveal the PIM power level caused by nonlinear MM contacts [5].

One of the difficulties when trying to locate PIM is that the nonlinearity that gives rise to them does not manifest itself at low input signal levels which is because PIM levels are normally low and at low power levels the PIMP may fall below the thermal noise level. Testing for PIM signal, measuring them and also locating sources can be a tough challenge for test equipment. So it's a more convenient and reasonable method to analyze and predict the PIM power level through the mathematical models to design the microwave devices and high frequency circuits.

The PIM power level of the nonlinear MM contact model is transformed into that of the nonlinear circuit. The harmonic balance method [6], the finite difference time domain (FDTD) method [7] and the large-signal-small-signal analysis method [8] are adopted to solve the nonlinear circuit. For instance, the advanced design system (ADS) is the electronic design software to analyze the I-V response of nonlinear circuits using the harmonic balance method [9]. The FDTD method, as a full wave

Submitted On: June 14, 2016
Accepted On: September 1, 2018

analysis, can analyze the current, voltage and electric field strength of nonlinear devices. Since it is a time-domain method, FDTD solutions can cover a wide frequency range with a single simulation run. What's more, FDTD calculates the E and H fields everywhere in the computational domain as they evolve in time. It lends itself to providing animated displays of the electromagnetic field movement through the model. The FDTD method is suitable to analyze the field-circuit coupling PIM problems with multiple carriers, nonlinearity, and wide frequency band characteristics.

This paper proposes a PIM analysis method of MM contacts based on the FDTD method. First, two nonlinear MM contact models are discussed. Second, the FDTD method for PIM analysis of nonlinear MM contacts is developed based on the power series and equivalent circuit models. Finally, two simulation examples are illustrated to verify the validity of the proposed method.

II. NONLINEAR MM CONTACT MODELS

Two mathematical models have been proposed to describe the nonlinear I-V characteristic of MM contacts. And the proposed mathematical models contribute to the calculation of PIM power level.

A. Power series model of nonlinear MM contacts

Assuming the microwave components with nonlinear MM contacts are excited by two signals with frequencies f_1 and f_2, an expression for its input voltage can be written as:

$$V_{in} = V_1 \cos(2\pi f_1 t) + V_2 \cos(2\pi f_2 t), \quad (1)$$

where V_{in} is the combined input signals, V_1 and V_2 are the amplitudes of two signals.

The transfer function of nonlinear passive components caused by MM contacts may be represented by the polynomial series method [10] as follows.

$$I = \sum_{k=0}^{K} a_k V_{in}^k, \quad (2)$$

where I is the total nonlinear current, a_k is the coefficient which depends on the nonlinear properties of components.

Substituting Eq. (1) into Eq. (2) and solving for all intermodulation and harmonic components of nonlinear current, we can get the spectrum of *I*. PIMP are generated at frequencies described by the following equation [11]:

$$f = mf_1 + nf_2, \quad (3)$$

where *m* and *n* can be negative as well as positive integers and the sum $|m|+|n|$ defines the order of the PIMP.

Once the I-V response curve of passive components with nonlinear MM contacts is measured, the spectrum of nonlinear current is easily transformed by the fast Fourier transformation (FFT). Then the PIM power level caused by nonlinear contacts can be calculated with the power series model.

B. Equivalent circuit model of nonlinear MM contacts

Due to the roughness of contact surfaces, the real contact occurs only at some points and the real contact area is much less than the nominal contact area. The MM micro-contact is shown in Fig. 1 [12, 13]. Two main regions including the contact and non-contact zones can be clearly differentiated. To reveal the electrical circuit characteristics of nonlinear MM contacts accurately, Vicente and Hartnagel established the equivalent circuit model [5].

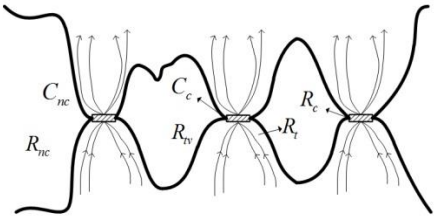

Fig. 1. Micro-schematic diagram of MM contact.

There exist some resistances and capacitances to describe the electrical characteristics of MM contact as shown in Fig. 2.

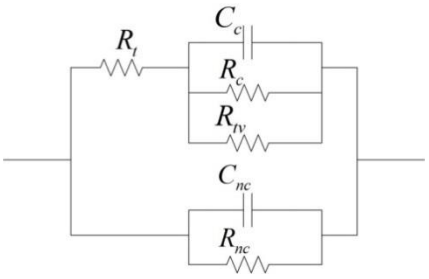

Fig. 2. Equivalent circuit of MM contact.

The constriction resistance R_t result from current constriction effect, it includes Maxwell resistance R_m and Sharvin resistance R_s. It can be calculated as follows:

$$R_t = f(\lambda / r_a)\frac{\rho}{2r_a} + \frac{4\rho\lambda}{3A_r}, \quad (4)$$

where $f(\lambda / r_a) = (1+0.83(\lambda / r_a)) / (1+1.33(\lambda / r_a))$ is interpolation function which revels the relationship between R_m and R_s λ is electron free path for the contact material, ρ is contact metal resistivity, $R_M = \rho / 2r_a$ is Maxwell resistance, $R_S = 4\rho\lambda / (3A_r)$ is Sharvin resistance. r_a is the average radius of the asperity contact circle, and A_r is real area of contact. The metal

contact resistance R_c, generates in contact zone because the outer adsorbed film cracks under the action of contact force. The formula for calculating the contact resistance R_c of asperity with a plurality of MM contact spots is as follows:

$$R_c = \frac{\rho}{2 r_{MM} N_c} f(\frac{r_{MM}}{r_a}), \tag{5}$$

where r_{MM} is the equivalent MM contact circle radius of a single asperity and N_c is the quantity of micro asperities, $f(r_{MM}/\bar{r}_a)$ is a function of the contraction scale considering the current constriction effect and it's expression is as follows:

$$f(\frac{r_{MM}}{\bar{r}_a}) = 1 - 1.41581(\frac{r_{MM}}{\bar{r}_a}) + 0.06322(\frac{r_{MM}}{\bar{r}_a})^2 + 0.15261(\frac{r_{MM}}{\bar{r}_a})^3 + 0.19998(\frac{r_{MM}}{\bar{r}_a})^4. \tag{6}$$

The tunnel resistance R_{tv} and contact capacitance C_c, produce in the zone that the adsorbed film does not crack. The tunnel resistance is based on tunnel current. The tunnel current density is nonlinear and voltage dependent. That is [14]:

$$R_{tv} = \frac{V}{A_S J_{tv}}, \qquad J_{tv} = \frac{e}{2\pi h s^2}(\varphi_0 e^{-4\pi\sqrt{\frac{2m\varphi_0}{h^2}}s} - (\varphi_0 + eV)e^{-4\pi\sqrt{\frac{2m(\varphi_0+eV)}{h^2}}s}), \tag{7}$$

where, J_{tv} is the tunnel current density, A_S is the tunnel area, φ_0 is the work function of metal, s is the thickness of barrier in the Fermi level, h is the Planck constant, *m* is the mass of electron. The tunnel current is the dominant nonlinear source in MM contact [15]. The contact capacitance is $C_c = \varepsilon_r \varepsilon_0 A_n A^* / s$, where ε_r is the relative dielectric constant of the insulating film on the metal, ε_0 is the vacuum dielectric constant, A_n is the nominal contact area and A^* is the dimensionless ratio of real contact area A_r and nominal contact area A_n. The non-contact resistance R_{nc} and the non-contact capacitance C_{nc} exist in the non-contact zone. The non-contact resistance is very large. The non-contact capacitance is $C_{nc} = \varepsilon_0 (A_n - A_r)/d$, where d is the distance of up and down non-contact area.

As shown in Fig. 1, in the contact zone, R_c, R_{tv} and C_c are parallel connection, and they are connected with the constriction resistance R_t in series. In the non-contact zone, R_{nc} and C_{nc} are connected in parallel. The non-contact resistance is very large, and the generation mechanism includes the field emission and the gas breakdown etc. The non-contact resistance can be regarded as an open circuit when analyzed. It can be seen from Fig. 1 that the circuits in the contact and non-contact zones are connected in parallel. Then, the equivalent circuit model of MM contact can be established as shown in Fig. 2, which can be used to describe the nonlinear I-V response of MM contact.

III. FDTD METHOD FOR PIM ANALYSIS OF NONLINEAR MM CONTACT

A. FDTD method for PIM analysis of power series model

The coaxial connector is as an example to illustrate the FDTD method for simulating the PIM power level of passive components. Coaxial connectors are one kind of common microwave components frequently used in communication system. Also they are the dominant contributors to PIM distortion in high frequency networks. Once the I-V response of connectors is measured, the PIM power level is conveniently calculated by FDTD method without considering the shape of connectors and PIM source location. When the PIM power level is simulated by FDTD, the I-V relationship of connectors can be taken as the I-V relationship of a lumped component in the FDTD meshes.

The lumped element at the node (i, j, k+1/2) and at time $t = (n+1/2)\Delta t$ can be derived by the Maxwell's curl-H equation as follows [4]:

$$E_z^{n+1}(i,j,k+\frac{1}{2}) = E_z^n(i,j,k+\frac{1}{2}) + \frac{\Delta t}{\varepsilon_0}(\nabla \times H)_z\Big|_{i,j,k+1/2}^{n+1/2} - \frac{\Delta t}{\varepsilon_0 \Delta x \Delta y} I_{zL}^{n+1/2}(i,j,k+\frac{1}{2}), \tag{8}$$

where Δt is the time step, ε_0 is the permittivity in vacuum.

The voltage $V_{zL}^{n+1/2}$ across the lumped element can be derived from the electric field E_z at the node (i, j, k+1/2) as follows:

$$V_{zL}^{n+1/2}\left(i,j,k+\frac{1}{2}\right) = \frac{\Delta z}{2}\left[E_z^{n+1}\left(i,j,k+\frac{1}{2}\right) + E_z^n\left(i,j,k+\frac{1}{2}\right)\right]. \tag{9}$$

Substituting Eq. (9) into Eq. (2), the current through the component can be expressed in discrete form as follows:

$$I_{zL}^{n+1}(i,j,k+\frac{1}{2}) = \sum_{k=0}^{K} a_k (\frac{1}{2}\Delta z (E_z^{n+1}(i,j,k+\frac{1}{2}) + E_z^n(i,j,k+\frac{1}{2})))^k. \tag{10}$$

Substituting Eq. (10) into Eq. (8), we can obtain the passive device's FDTD iterative formula of electric field at the node (i, j, k+1/2) as follows:

$$E_z^{n+1}(i,j,k+\frac{1}{2}) = E_z^n(i,j,k+\frac{1}{2}) + \frac{\Delta t}{\varepsilon_0}(\nabla\times H)_z\Big|_{i,j,k+1/2}^{n+1/2} - \frac{\Delta t}{\varepsilon_0\Delta x\Delta y}\sum_{q=0}^{w} a_q(\frac{1}{2}\Delta z(E_z^{n+1}(i,j,k+\frac{1}{2}) + \frac{1}{2}E_z^n(i,j,k+\frac{1}{2})))^q. \quad (11)$$

Then the nonlinear current of passive device is calculated as follows:

$$\begin{cases} J = \sigma E \\ I = J\Delta x\Delta y \end{cases}, \quad (12)$$

where J is the current density, σ is the conductivity.

The obtained time domain current I is transformed to frequency domain by FFT. Finally the PIM power level with frequency of f is calculated as follows:

$$P_f = I_f^2 Z, \quad (13)$$

where I_f is the current amplitude with frequency of f, Z is the resultant impedance of lumped circuit.

B. FDTD method for PIM analysis of equivalent circuit model

The FDTD iterative formula of each element in equivalent circuit model should be derived firstly. Then all FDTD iterative formulas of elements are combined according to the topology of equivalent circuit. If the lumped element is a constriction resistance or contact resistance, the current through the liner resistance is:

$$I_{zL}^{n+\frac{1}{2}}(i,j,k+\frac{1}{2}) = \frac{V_{zL}^{n+\frac{1}{2}}(i,j,k+\frac{1}{2})}{R}, \quad (14)$$

where V_{zL} is the voltage across the lumped element, R is the constriction resistance R_t or contact resistance R_c.

The relationship between V_{zL} and the electric field E_z at the node (i, j, k+1/2) is as shown in Eq. (9).

Substituting Eqs. (9) and (14) into Eq. (8), we can obtain the resistor's FDTD iterative formula of electric field at the node (i, j, k+1/2) as follows:

$$E_z^{n+1}(i,j,k+\frac{1}{2}) = \frac{1-\frac{\Delta t\Delta z}{2R\varepsilon_0\Delta x\Delta y}}{1+\frac{\Delta t\Delta z}{2R\varepsilon_0\Delta x\Delta y}}E_z^n(i,j,k+\frac{1}{2}) + \frac{\Delta t/\varepsilon_0}{1+\frac{\Delta t\Delta z}{2R\varepsilon_0\Delta x\Delta y}}(\nabla\times H)_z\Big|_{i,j,k+1/2}^{n+1/2}. \quad (15)$$

If the lumped element is a contact capacitance or non-contact capacitance, the current through the capacitance is:

$$I_C = C\frac{dU}{dt}, \quad (16)$$

where C is contact capacitance or non-contact capacitance, U is the voltage across the capacitance.

The relationship between the I and E_z at the node (i, j, k+1/2) is:

$$I_{zL}^{n+1/2}(i,j,k+\frac{1}{2}) = \frac{C\Delta z}{\Delta t}(E_z^{n+1}(i,j,k+\frac{1}{2}) - E_z^n(i,j,k+\frac{1}{2})). \quad (17)$$

Substituting Eq. (17) into Eq. (8), we can obtain the capacity's FDTD iterative formula of electric field at the node (i, j, k+1/2) as follows:

$$E_z^{n+1}(i,j,k+\frac{1}{2}) = E_z^n(i,j,k+\frac{1}{2}) + \frac{\Delta t/\varepsilon_0}{1+\frac{C\Delta z}{\varepsilon_0\Delta x\Delta y}_z}(\nabla\times H)_z\Big|_{i,j,k+1/2}^{n+1/2}. \quad (18)$$

For the tunnel resistance, the relationship between the voltage and electric field of tunnel resistance at the node (i, j, k+1/2) is as shown in Eq. (9).

Substituting Eqs. (7) and (9) into Eq. (8), we can obtain the tunnel resistance's FDTD iterative formula of electric field at the loaded node as follows:

$$E_z^{n+1}(i,j,k+\frac{1}{2}) = E_z^n(i,j,k+\frac{1}{2}) + \frac{\Delta t}{\varepsilon_0}(\nabla\times H)_z\Big|_{i,j,k+1/2}^{n+1/2} - J_{tv}^{n+1}(i,j,k+\frac{1}{2}). \quad (19)$$

According to the above analysis of lumped elements, we may calculate the circuit shown in Fig. 2 and obtain the nonlinear current through the MM contact in Matlab software [16].

When the equivalent circuit model reveals the I-V relationship of nonlinear MM contacts in high frequency circuit, the PIM power level can be calculated by Eqs. (12) and (13). However, like as wire mesh reflectors, the PIM sources caused by nonlinear MM contacts can also be modeled in equivalent circuit, and the PIM power level transmitted by mesh reflectors can be simulated by FDTD. Firstly, the nonlinear current through the MM contacts is calculated by FDTD. Secondly, the calculated nonlinear current is regarded as the excitation source to simulate the PIM scattered field of the far field in FDTD method. Finally, the PIM scattered field of the far field is transformed to PIM power level of mesh reflectors by Friis transmission equation.

IV. SIMULATION EXAMPLES AND VERIFICATION

A. PIM simulation of power series model

The nonlinear I-V relationship of a passive device may be described by power series. The nonlinear current through the passive device is calculated by Eq. (11) and

(12). The PIM power level is determined by Eq. (13).

For instance, an N-type coaxial connector, as shown in Fig. 3, is used to evaluate the 3rd-order PIM power level by the proposed method and experimental test. The Rosenberger IM-26P PIM analyzer is used to measure the 3rd-order PIM power level of the coaxial connector which is excited by two signals with the frequencies of 2.62GHz and 2.69GHz in a reflection configuration at 43dBm input power, as shown in Fig. 4. The measured result is -99.8dBm.

Fig. 3. An N-type coaxial connector.

The nonlinear I-V characteristic of the N-type coaxial connector is measured and then expressed by a 3rd order power series as follows:

$$I = -10.081V^3 - 12.9439V^2 + 5.4809V - 9.4723\times10^{-4}. \quad (20)$$

Combining Eqs. (11), (12), (13) and (20), the PIM power levels of the coaxial connector calculated by the proposed FDTD method are illustrated in Fig. 5. The 3rd-order PIM power level is -103.2 dBm. The error of the 3rd-order PIM power level is 3.4 dB compared with the test result, which sufficiently shows the accuracy of the proposed FDTD method. It can be concluded that the FDTD method for PIM analysis of MM contacts can address the field-circuit coupling electromagnetism simulation problem, which offers a solution for the PIM analysis of mesh reflectors as described below.

Fig. 4. A measuring system composed of a PIM analyzer, a computer and device under test.

B. PIM analysis of MM contacts in mesh reflectors

The mesh reflector is made of three wires of tungsten (twisted together) with an individual core diameter of 15 microns. The overcoat covering each micro-wire is made of gold (thickness of 0.25 micron) lying over an intermediate layer of nickel (thickness of 0.2 micron). These loose MM contact points of mesh reflectors belonging to contact nonlinearities are important PIM sources. The dimension of the wire mesh sample measured is 1m×1m. The sample shown in Fig. 6 has a nominal tension of 300g/m. The frequencies of the carriers are 2.16GHz and 2.21GHz with a power of 43dBm. The result of a PIM test in the radiated mode indicates the seventh-order PIM value of the sample is -139dBm.

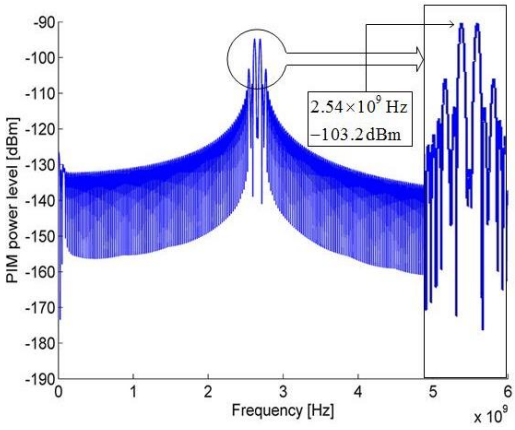

Fig. 5. PIM power levels evaluated by the proposed FDTD method.

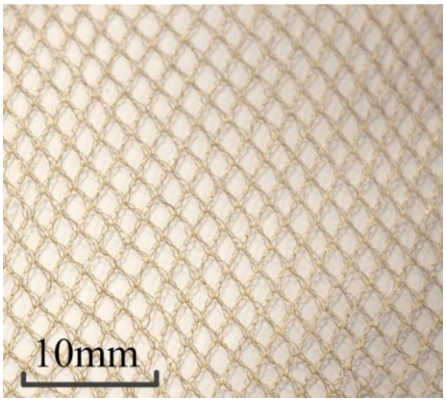

Fig. 6. Wire mesh sample.

There exists the gold-gold contact between two wires. The Poisson's ratio, elastic modulus, hardness, and resistivity of gold are 0.42, 79GPa, 275MPa, and $2.4\times10^{-8}\Omega$m, respectively. The mean free path of electrons is 38nm. The parameters of metal surface include the micro-asperity density $\eta = 7\times10^{15}/\text{m}^2$, the standard deviation of

surface height σ =5nm, the mean of asperity height z=8nm, and the relative dielectric constant ε_r =3. As shown in Fig. 7, the FEM model of wire mesh unit is established in ANSYS software, and the contact force and actual contact area can be obtained from the simulation result. The parameters are used to calculate R_t, R_c, C_c, C_{nc}, and R_{tv} in the equivalent circuit.

The contact force of single junction of wire mesh is calculated by fractal mechanics [17]. The parameters of circuit elements in the equivalent circuit model are calculated according to the contact force and the material parameters based on the expressions of each element in the equivalent circuit shown in Fig. 2. For example, if the contact force of two wire mesh is 5×10^{-8}N, the nonlinear current through the contact junction is calculated by the FDTD method shown in Fig. 8.

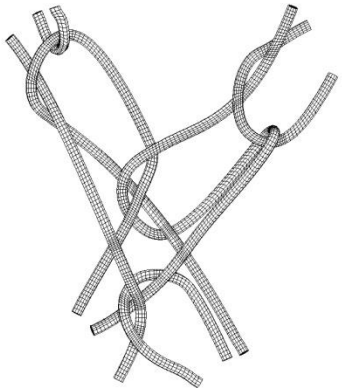

Fig. 7. The FEM model of wire mesh unit.

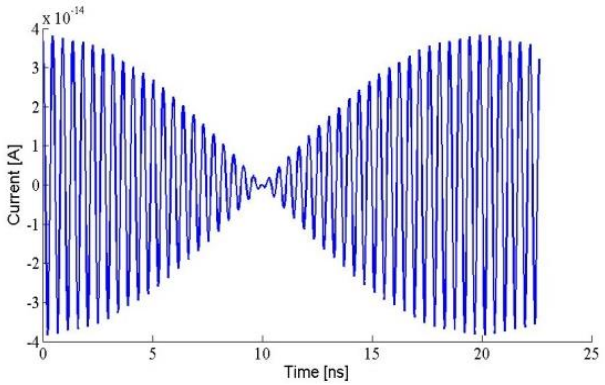

Fig. 8. Nonlinear current through the MM contact point.

Based on the nonlinear currents through contact junction, the far-field PIM power level of wire mesh can be simulated by the FDTD method. The analytical procedure is as follows:

(1) Taking the nonlinear current as a new electromagnetic wave source such as monopole antenna, the scattered field of the far field can be obtained by the FDTD method.

(2) The calculated time-domain electric field intensity is converted into the frequency-domain one by FFT. In the form of absolute amplitude, the electric field intensity E of the scattered field is 10lgE with a unit of $dB\mu V/m$.

(3) The far-field scattered field is an electric field E with a unit of $\mu V/m$, while the resulted analysis is to obtain the PIM power level P_r with a unit of mW. The transformation relationship between E and P_r is as follows [18]:

$$10\lg P_r = 20\lg E - 20\lg f + 10\lg G_r - 77.21, \quad (21)$$

where G_r is the gain of antenna.

(4) Consider all contact junctions of wire mesh in the most serious cases of the independent and phase uncorrelated PIM source, the received PIM power with a unit of dBm is:

$$P_f = 10\lg(P_{r1} + P_{r2} + \cdots + P_{rN}), \quad (22)$$

where P_{ri} $(i = 1, 2, \cdots, N)$ is the PIM power level arising from the ith contact point, N is the total number of contact points in the wire mesh.

As shown in Fig. 6, the mesh reflector is composed of many weaving units, one of which is shown in Fig. 7. Each weaving unit contains 18 contact junctions. According to the direction of force acting on the contact junction, the junctions are classified into two categories, in plane and out of plane. The nonlinear current is calculated through each contact junction. However, there exist millions of contact junctions in mesh reflectors. The computing scale is too huge to calculate. Because the size of the weaving unit is far smaller than the wavelength, the phase difference caused by the positions of contact junctions can be ignored. Hence, the equivalent current of monopole antenna is the sum of same category contact junctions in the weaving unit. As shown in Fig. 9, the nonlinear currents existing in a weaving unit are equivalent to two emitters.

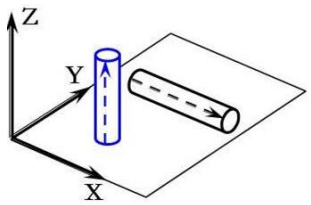

Fig. 9. Two equivalent emitters.

We consider the symmetry of wire mesh and the limitation of computing resources, we divide one quarter of the whole wire mesh into 19 groups and there are 82 weaving units in each group.

According to the above analytical procedure, the scattered field of the nonlinear current shown in Fig. 8 is obtained by Eq. (21), as shown in Fig. 10. The corresponding 7th-order PIM power level is -346.50 dBm. For the 1m×1m wire mesh, the 7th-order PIM power level is -130.77dBm by Eq. (22). The error is 5.9% compared with the test result -139dBm, which sufficiently validate the feasibility of the proposed approach.

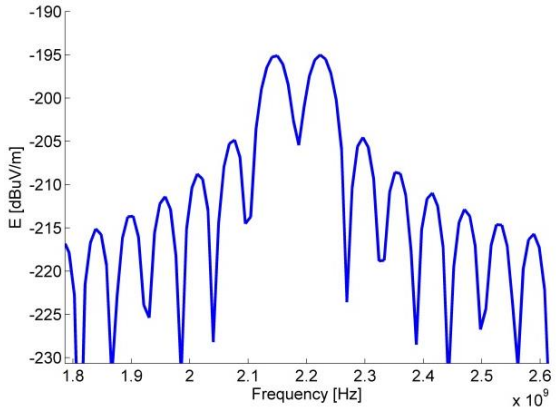

Fig. 10. Frequency-domain scattered field of the MM contact junction.

V. CONCLUSION

(1) The nonlinear MM contact is described by the power series model and equivalent circuit model respectively. The FDTD iterative formulas of two models are derived.

(2) The nonlinear current and PIM power level of power series model are developed by the FDTD method. The simulation and test results show the feasibility of the FDTD method.

(3) The nonlinear MM contact of mesh reflector is represented as the equivalent circuit model. The nonlinear current and PIM power level of wire mesh are solved by the FDTD method. The simulation result indicates the effectiveness of the proposed FDTD method which is suitable for solving the field-circuit coupling PIM problem.

ACKNOWLEDGMENT

The authors thank the anonymous reviewers for their valuable comments on the manuscript. This research was supported by the National Natural Science Foundation of China (Grant No. U1537213 and 61801175).

REFERENCES

[1] P. L. Lui and A. D. Rawlins, "Passive non-linearities in antenna systems," *IEE Colloquium on Passive Intermodulation Products in Antennas & Related Structures*, London, pp. 6/1-6/7, 1989.

[2] F. Arazm and F. A. Benson, "Nonlinearities in metal contacts at microwave frequencies," *IEEE Transactions on Electromagnetic Compatibility*, vol. EMC-22, no. 3, pp. 142-149, 1980.

[3] J. Jiang, T. J. Li, and Y. C. Liu, "Passive inter-modulation scattering analysis of reflector considering contact nonlinearity," *Chinese Journal of Aeronautics*, vol. 26, no. 2, pp. 463-469, 2013.

[4] W. Sui, D. A. Christensen, and C. H. Durney, "Extending the two-dimensional FDTD method to hybrid electromagnetic systems with active and passive lumped elements," *IEEE Transactions on Microwave Theory Techniques*, vol. 40, no. 4, pp. 724-730, 1992.

[5] C. Vicente and H. L. Hartnagel, "Passive-inter-modulation analysis between rough rectangular waveguide flanges," *IEEE Transactions on Microwave Theory & Techniques*, vol. 53, no. 8, pp. 2515-2525, 2005.

[6] F. N. Zghoul, "*Analyzing single and multitone nonlinear circuits using a modified harmonic balance method*," University of Idaho, Idaho, 2006.

[7] P. Ciampolini, P. Mezzanotte, L. Roselli, and R. Sorrentino, "Accurate and efficient circuit simulation with lumped-element FDTD technique," *IEEE Transactions on Microwave Theory and Techniques*, vol. 44, no. 12, pp. 2207-2215, 1996.

[8] H. Jokinen, "Computation of the steady-state solution of nonlinear circuits with time-domain and large-signal-small-signal analysis methods," *Acta Polytechnica Scandinavica Electrical Engineering*, vol. 87, pp. 1-75, 1997.

[9] B. R. Poole, S. D. Nelson, and S. Langdon, "Advanced electric and magnetic material models for FDTD electromagnetic codes," *Particle Accelerator Conference*, Knoxville, Tennessee, pp. 2639-2680, 2005.

[10] V. Golikov, S. Hienonen, and P. Vainikainen, "Passive intermodulation distortion measurements in mobile communication antennas," *IEEE 54th Vehicular Technology Conference*, vol. 4, pp. 2623-2625, 2001.

[11] J. Jiang, T. J. Li, and X. F. Ma, "A nonlinear equivalent circuit method for analysis of passive intermodulation of mesh reflectors," *Chinese Journal of Aeronautics*, vol. 27, no. 4, pp. 924-926. 2014.

[12] S. A. Maas, *Nonlinear Microwave and RF Circuits*. Artech House Publishers, Norwood, MA, 2003.

[13] O. Rezvanian, M. A. Zikry, C. Brown, and J. Krim, "Surface roughness, asperity contact and gold RF MEMS switch behavior," *Journal of Micromechanics and Microengineering*, vol. 19, no. 10, pp. 2006-2015, 2007.

[14] J. G. Simmons, "Generalized formula for the electric tunnel effect between similar electrodes separated by a thin insulating film," *Journal of*

Applied Physics, vol. 34, no. 6, pp. 1973-1803, 1963.

[15] M. Vladimirescu, R. Kwiatkowski, and K. Engel, "Passive intermodulation distortion in RF coaxial electro-mechanical switches for space applications," *The 4th International ESA Multipactor, Corona and Passive Intermodulation Workshop*, Noordwijk, Netherlands, 2003.

[16] A. Z. Elsherbeni and V. Demir, *The Finite-Difference Time-Domain Method for Electromagnetics with MATLAB Simulations*. 2nd edition, The SciTech Publishing, UK, 2015.

[17] T. J. Li, J. Jiang, T. T. Shen, and Z. W. Wang, "Analysis of mechanical properties of wire mesh for mesh reflectors by fractal mechanics," *International Journal of Mechanical Sciences*, vol. 92, no. 3, pp. 90-97, 2015.

[18] S. Y. Liao, "Measurements and computations of electric field intensity and power density," *IEEE Transactions on Instrumentation & Measurement*, vol. 26, no, 1, pp. 53-57, 1977.

Tuanjie Li received his Ph.D. degree from Xi'an University of Technology in 1999. He now is a Professor and Ph.D. Supervisor at School of Mechano-electronic Engineering, Xidian University. His main research interests are space deployable structures and passive intermodulation.

Wangmin Zhai received his diploma in 2017 from Xidian University. He now is a master of Mechanical Engineering in Xidian University. His current research interests include microwave technique and passive intermodulation.